EUROPEAN COMMISSION

nuclear science and technology

Structural Margin Improvements in Age-embrittled RPVs with Load History Effects (SMILE)

Editors: D. Moinereau and G. Bezdikian, EDF (FR)

Contract FIKS-CT2001-00131

Final report

Work performed as part of the European Atomic Energy Community's research and training programme in the field of nuclear energy 1998-2002 (Fifth Framework Programme)
Key action: Nuclear fission
Area: Operational safety of existing installations

Directorate-General for Research
2008 Euratom EUR 23317

Project coordinator

Électricité de France (FR)

Project partners

D. Moinereau [1], G. Bezdikian [2], A. Dahl [3], Y. Wadier [4], P. Gilles [5], E. Keim [6], S. Chapuliot [7], T. Yuritzinn [8], B. Marini [9], N. Taylor [10], D. Siegele [11], L. Streibig [12], D. Arnaud [14], G. Nagel [15], P. Budden [16], R. Bass [17], K. Kerkhof [18], D. Lidbury [19], J. Sharples [20]

[1] EDF R&D, dominique.moinereau@edf.fr
[2] EDF DPN, georges.bezdikian@edf.fr
[3] EDF R&D, anna.dahl@edf.fr
[4] EDF R&D, yves.wadier@edf.fr
[5] AREVA, philippe.gilles@areva.com
[6] AREVA, elisabeth.keim@areva.com
[7] CEA, stephane.chapuliot@cea.fr
[8] CEA, tamara.yuritzinn@cea.fr
[9] CEA, bernard.marini@cea.fr
[10] JRC-IE, nigel.taylor@cec.eu.int
[11] IWM Freiburg, si@iwm.fhg.de
[12] BCCN, laurent.streibig@asn.minefi.gouv.fr
[14] BCCN, dominique.arnaud@asn.minefi.gouv.fr
[15] E.ON, gerhard.nagel@eon-energie.com
[16] British Energy, peter.budden@british-energy.com
[17] ORNL, bassbr@ornl.gov
[18] MPA Stuttgart, klaus.kerkhof@mpa-uni.stuttgart.de
[19] Serco, david.lidbury@serco.com
[20] Serco, john.sharples@sercoassurance.com

CONTENTS

1. INTRODUCTION

The SMILE project started in January 2002, as part of the Fifth Framework Programme of the European Atomic Energy Community (Euratom FP5), and is now achieved [1]. It aims at confirming on small- and large-scale specimens the beneficial effect of warm pre-stress (WPS) in RPV assessment leading to a significant improvement of the material resistance regarding the risk of brittle failure, and to model and validate this effect. It also aims at harmonising the different approaches to lay the basis for European codes and standards regarding the inclusion of WPS in RPV assessment regarding the risk of brittle failure.

Within the framework of the project, main experimental, analytical, and numerical results are now available. They are summarised in this report. Based on these results, some recommendations are proposed for the application and inclusion of WPS in RPV safety assessments.

2. WARM PRE-STRESS AND RPV ASSESSMENT

2.1 Terminology

The following symbols are used in this report:

t	time
RPV	reactor pressure vessel
PTS	pressurised thermal shock
WPS	warm pre-stress
K_{WPS}	stress-intensity factor due to pre-loading
K_{unload}	stress-intensity factor following unloading
LCF	load-cool fracture cycle (loading path)
LTF	load-transient fracture cycle (loading path)
LCUF	load-cool-unload fracture (loading path)
LUCF	load-unload-cool fracture (loading path)
T_1	temperature at pre-loading
T_2	temperature at reloading
K_J	stress-intensity factor (crack driving force)
K_{Ic}	material fracture toughness (generally measured on CT specimens)
K_{FRAC}	stress-intensity factor at final failure
ΔK_U	range of stress-intensity factor due to unloading ($\Delta K_U = K_{WPS} - K_{unload}$)
ΔK_R	range of stress-intensity factor due to reloading ($\Delta K_R = K_{FRAC} - K_{unload}$)
β	plasticity correction factor
σ_Y	yield stress at pre-loading conditions

2.2 Description of warm pre-stress

The warm pre-stress phenomenon is well known regarding the risk of RPV brittle failure for ferritic steels during possible overcooling PTS transient.

'A warm pre-stress (WPS) is an initial pre-loading applied to a ferritic steel containing a pre-existing flaw which is carried out at a temperature above the ductile-brittle transition temperature, and at a higher temperature or in a less embrittled state than that corresponding to the subsequent service assessment' [R6 – Revision 4, Chapter III, Section III.10.4]. *Failure is avoided if the stress-intensity factor during cooling is constant or monotonically falling, even if crossing between K_{Ic} curve and K_J load path.*

From a practical point of view, the WPS effect induces two major consequences regarding the risk of RPV brittle failure during a PTS transient:

– Brittle failure is impossible during the unloading (decreasing of the stress-intensity factor K_J).

– In case of a final additional reloading of the vessel at lower temperature, brittle failure would be obtained with additional margins (K_{FRAC}) compared to initial material fracture toughness (K_{Ic}), as summarised below.

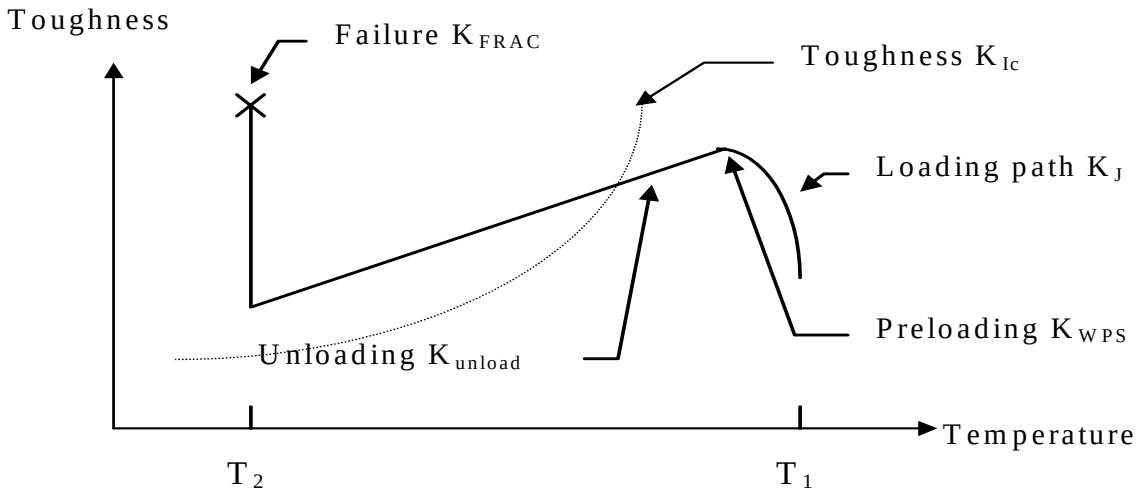

Figure 1: WPS principle

The explanations generally attributed to this effect are establishment – during the loading path – of a compressive residual stress zone ahead of the crack tip, crack tip blunting, and strain hardening.

2.3 Practical application in RPV assessment

In a deterministic approach, the RPV safety assessment is generally based on the comparison between the stress-intensity factor K_J and the material fracture toughness K_{Ic}, including some safety factors. It is for example the case in French RCCM and RSEM codes, with a comparison $K_J - K_{Ic}$ and the respect of required safety factors during the entire transient (including loading and unloading phases of the loading path).

Several configurations can be met, as described in the following schematic, showing sometimes a significant impact of WPS on the RPV assessment and the corresponding margins.

Configuration 1

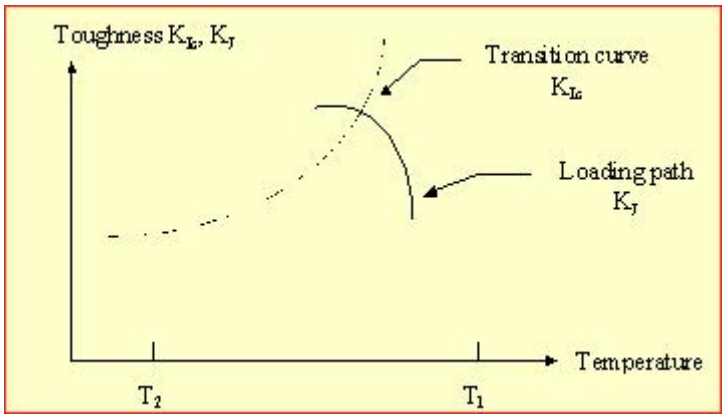

Figure 2: Example of loading path

There is no possible WPS effect, due to monotonic increasing loading (K_J).

Configuration 2

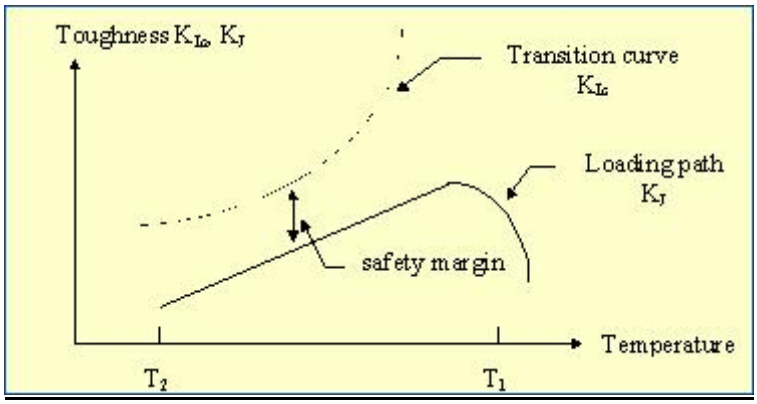

Figure 3: Example of loading path

The stress-intensity factor (K_J) is always lower than the material fracture toughness (K_{Ic}), brittle initiation is not possible due to unloading (WPS). However, some margins can be required in some codes during all transient, in spite of unloading.

Configuration 3

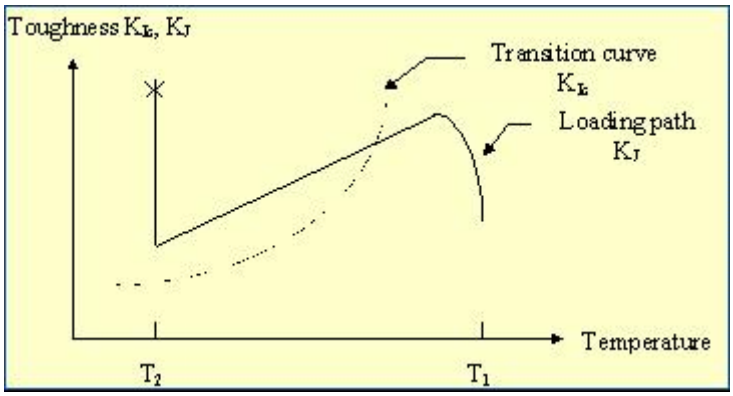

Figure 4: Example of loading path

During cooling, the stress-intensity factor (K_J) becomes greater than the material fracture toughness (K_{Ic}). Due to WPS effect, brittle initiation is not possible during the unloading part of the transient and can occur only in case of additional reloading at lower temperature. If WPS is not taken into account, brittle initiation will occur before, during unloading.

Configuration 4

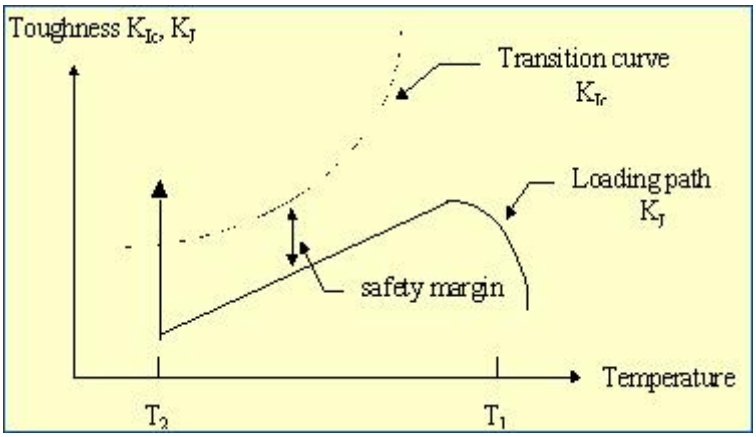

Figure 5: Example of loading path

This scenario is a combination of previous configurations 2 and 3. The stress-intensity factor (K_J) is still lower than the material fracture toughness (K_{Ic}), brittle initiation is not possible due to unloading (WPS) and can occur only in case of additional reloading at lower temperature ($K_J > K_{Ic}$). However, some margins can be required in some codes during all transient, and more particularly during the unloading phase, in spite of unloading.

2.4 Present status of warm pre-stress in Codes & Standards

Inclusion of warm pre-stress concept in Codes & Standards, as well as effective practice in RPV safety assessment, is variable according to codes and national requirements, as shown below (limited to SMILE scope):

USA (ASME code)

According to Appendix A of Section XI, Article A-5400, Emergency and faulted conditions (very low probability postulated incidents whose consequences are such that subsequent plant operation is not required and safe system shutdown is the only consideration), WPS is applicable to the following conditions (7):

For those transients where K_I is monotonically decreasing with time (e.g. where system repressurization is limited), warm prestressing may be credited to preclude flaw initiation or reinitiation at times in the transient beyond the time of the peak stress-intensity factor.

The WPS concept is included in the probabilistic code FAVOR.

Germany (KTA rules)

The WPS concept is included in German KTA Rule 3201.2, Paragraph 7.9 'Brittle failure analysis', and has been already applied in flaw assessment. There is no limitation for preloading. The criterion for WPS is $dK/dt \leq 0$.

United Kingdom

The flaw assessment is based on the failure assessment diagram (FAD) in the R6 procedure; there is no direct comparison between the material fracture toughness and the stress-intensity factor (or driving force). The warm pre-stress effect is included in R6 flaw assessment procedure, the advice in British Standard flaw assessment document BS7910 taken from R6. The WPS is not included in UK design codes. No use has been made of a quantitative WPS model; the only use has been of the conservative WPS principle. The UK regulator, NII, has accepted cases made according to this conservative WPS principle.

France (RCCM & RSEM codes)

The WPS concept is not included in present codes RCCM (Design) and RSEM (In-service assessment) and cannot be used in RPV assessment.

Experimental evidence of warm pre-stress has been widely demonstrated in the past. However, up to now, capability of available models to demonstrate this effect and to evaluate and quantify additional margins induced by such an effect has never been demonstrated.

3. OBJECTIVES AND ORGANISATION OF THE SMILE PROJECT

The organisation of SMILE project is summarised in the following table, including six work packages:

WP1	**Co-ordination and management**	**EDF**
WP2	**Calibration tests** **WP2.1** Characterisation of the degraded material **WP2.2** Confirmation of the WPS effect on degraded material (WPS3) **WP2.3** Calibration of WPS models on undegraded material (18MND5) **WP2.4** Load history effect on ductile tearing	**SERCO**
WP3	**Assessment of models** **WP3.1** Selection of models **WP3.2** Validation of models against existing data (WPS3 & 18MND5)	**CEA**
WP4	**Validation test** **WP4.1** Test specification and design of test **WP4.2** Validation test **WP4.3** Fractography **WP4.4** Interpretation of validation test	**MPA**
WP5	**Cases studies** **WP5.1** Development of cases studies specifications **WP5.2** Application to a RPV subclad flaw with an actual PTS transient **WP5.3** Application to a RPV through clad surface crack with an actual PTS transient	**Framatome-ANP GmbH**
WP6	**Programme evaluation, synthesis and recommendations** **WP6.1** Guidelines for Codes & Standards **WP6.2** Conclusions and recommendations	**EDF**

Table 1: SMILE project

The main objectives of the project are summarised as follows:

– A description of the state of art regarding WPS in RPV assessment, including modelling

– A deeper demonstration and understanding of the WPS effect, through experimental works on CT specimens and a 'large-scale' WPS-type experiment on a cracked cylinder

– A validation of analytical and numerical models through benchmarks and analyses of WPS experiments

– Some applications to real European RPVs

– An establishment of recommendations concerning use and application in real industrial cases

– A final draft giving guidelines and recommendations in Design & Regulatory Codes and Standards.

More details and information concerning SMILE project are available in documents [1][2][3]. The deliverables of the project (D1 to D15) are mentioned in references [4] to [18].

4. SYNTHESIS OF SMILE RESULTS

4.1 Experimental results

WPS effect has been experimentally studied on two materials:

– WPS3 steel (17MoV8-4mod. steel) (MPA Stuttgart): heat-treated material in order to simulate an end-of-life (EOL) RPV material (high $RT_{NDT} - T_0$:140°C, low upper shelf …)

– 18MND5 steel (plate material similar to A533 steel) (EDF): fully representative of unirradiated RPV steel (begin of life).

The experimental part of the project is fully achieved. All experimental results are available on both materials, including materials characterisation and WPS-type experiments conducted on classical CT specimens (18MND5 & WPS3 steels) and on one large-scale cracked cylinder (17MoV8-4 mod. steel (WPS3)). All corresponding data and results are available in documents [4][5][6][7][8][10][11][12] and [13].

4.1.1 WPS experiments on CT specimens

The effect of WPS has been studied on the material resistance regarding the risk of brittle failure, using classical WPS type experiments performed on conventional CT specimens (1T, 2T and 4T CT specimens). The experiments have been conducted on both materials (18MND5, WPS3) with several classical WPS loading paths (K_J – T cycles): LCF, LUCF, LTF …

Main experimental conditions of the experiments are summarised in the following table:

Material	**T_{WPS}**	**T_{FRAC}**	**Preloading K_{WPS} MPa.m$^{0.5}$**	**WPS cycles**
WPS3 (17MoV8-4 mod.) (MPA)	280 °C	20 °C	80	LCF LUCF …
18MND5 (EDF)	20 °C	– 150 °C	60	LCF LUCF …
18MND5 (EDF)	20 °C	– 150 °C	100	LCF LUCF …

Table 2: Test matrix on CT specimens

Experimental results obtained on CT specimens for both materials are summarised in the following figures:

WPS3 material (17MoV8-4mod. steel)

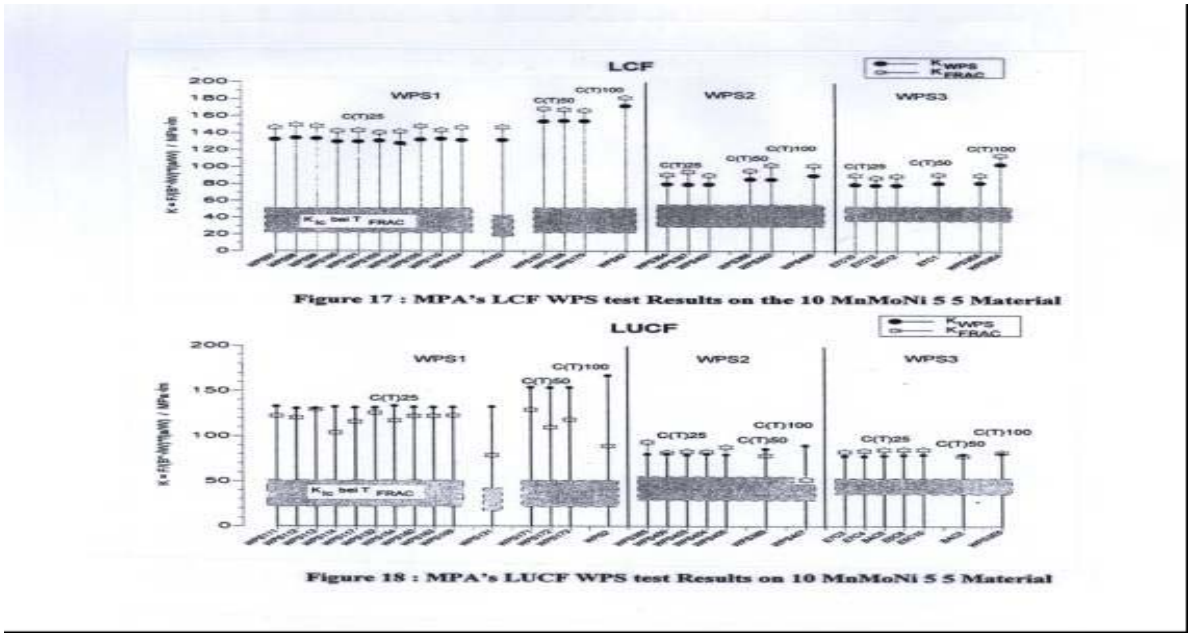

Figure 17 : MPA's LCF WPS test Results on the 10 MnMoNi 5 5 Material

Figure 18 : MPA's LUCF WPS test Results on 10 MnMoNi 5 5 Material

Figure 6a: Experimental results on WPS3 material

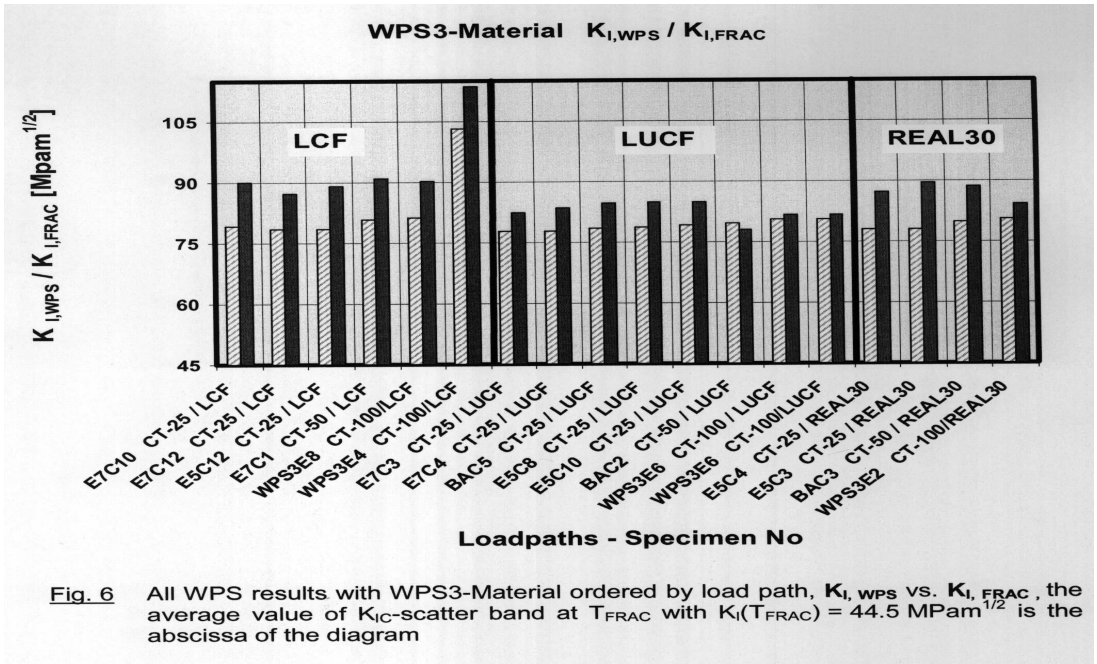

Fig. 6 All WPS results with WPS3-Material ordered by load path, $K_{I,WPS}$ vs. $K_{I,FRAC}$, the average value of K_{IC}-scatter band at T_{FRAC} with $K_I(T_{FRAC})$ = 44.5 MPam$^{1/2}$ is the abscissa of the diagram

Figure 6b: Experimental results on WPS3 material (details) ($K_{I,WPS}$ in grey, $K_{I,FRAC}$ in black)

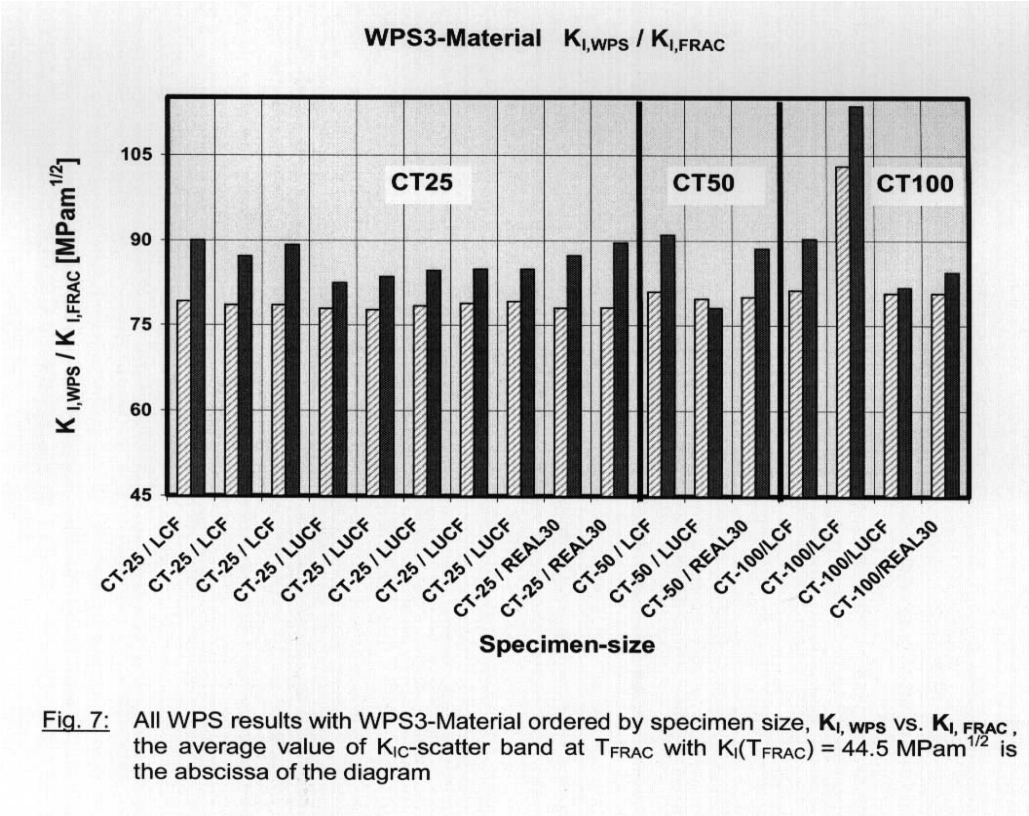

Fig. 7: All WPS results with WPS3-Material ordered by specimen size, $K_{I,WPS}$ vs. $K_{I,FRAC}$, the average value of K_{IC}-scatter band at T_{FRAC} with $K_I(T_{FRAC})$ = 44.5 MPam$^{1/2}$ is the abscissa of the diagram

Figure 6c: Experimental results on WPS3 material (details) ($K_{I,WPS}$ in grey, $K_{I,FRAC}$ in black)

18MND5 material (similar to A533 steel)

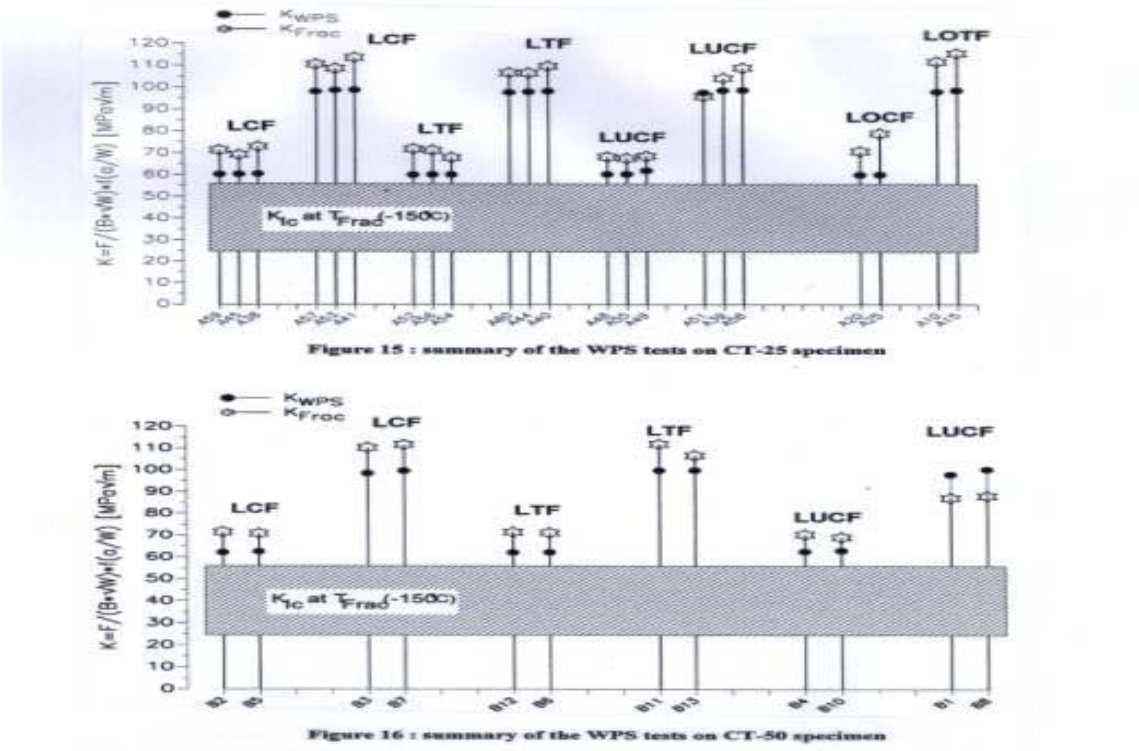

Figure 7: Experimental results on 18MND5 material

From a qualitative point of view, all the results clearly confirm the beneficial effect of warm pre-stress on the materials resistance regarding the risk of brittle failure:

– No initiation occurred during unloading ($dK_J/dt < 0$), whatever the scenarios (material, loading path, level of preloading …), even if $K_J > K_{Ic}$

– No initiation occurred during cooling with constant loading ($dK_J/dt = 0$ (e.g. LCF cycles)), even if $K_J > K_{Ic}$

– In case of an additional reloading at lower temperature, a significant increase of material resistance at failure (K_{FRAC}) is obtained regarding the risk of brittle failure initiation, compared to the initial material fracture toughness K_{Ic} (in the absence of the WPS)($K_{FRAC} > K_{Ic}$ or $K_{FRAC} >> K_{Ic}$, according the loading path K_J-T).

From a quantitative point of view, the margins induced by WPS on the material resistance (K_{FRAC}/K_{Ic}) are influenced by the level of preloading (K_{WPS}) and the type of WPS cycle [19].

4.1.2 WPS-type experiment on a cracked cylinder (WPS3 material)

In order to demonstrate WPS effect on a 'real component' under PTS conditions, a WPS type experiment has been conducted by MPA Stuttgart on a cracked cylinder submitted to a more complex loading simulating a PTS event on a RPV.

A schematic of the test is given below, but full details about the experiment are available in documents [4][5][11][12][13]:

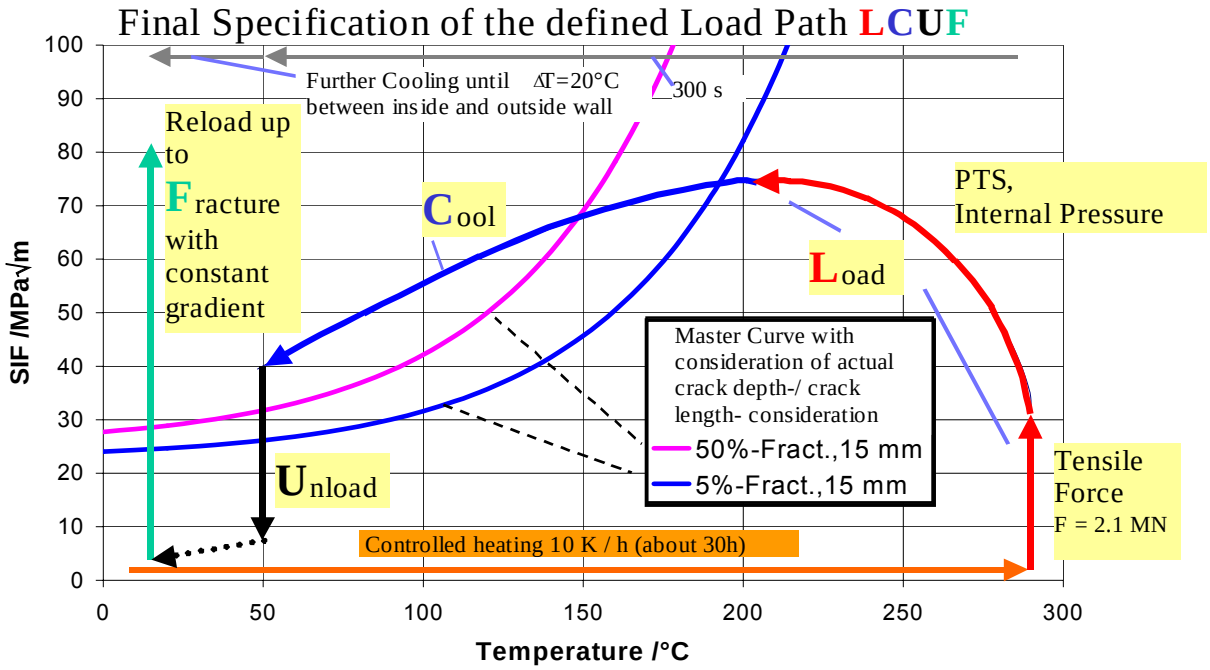

Figure 8: Specification of loading path for WPS experiment on cracked cylinder

The experiment was conducted as follows:

– Pronounced pre-loading in the upper shelf region without ductile tearing initiation

– Thermal shock by internal cooling of the specimen

– No fracture expected during cooling phase, although crossing of fracture toughness K_{Ic} and decreasing stress-intensity factor K_J curves

– Final tensile reloading of the specimen at room temperature up to final failure (with expected brittle failure).

The experiment has been conducted with full success and all objectives have been reached. Main conclusions of the experiment can be summarised as follows:

– No failure event occurred during the unloading cooling phase, although K_J curve crossing the K_{Ic} fracture toughness curve in the transition region

– Brittle failure of the cylinder was obtained during the final tensile reloading of the cylinder with a high level of loading

– A significant increase of the cylinder resistance is observed compared to the initial material fracture toughness.

The final synthesis of analyses is available in Deliverable [14]. The results, showing a significant improvement of the component resistance regarding brittle failure due to WPS compared to original material fracture toughness, are summarised below. Notice also that the stress-intensity factor at failure, K_{FRAC}, is slightly above the level of initial preloading K_{WPS}:

	K_{FRAC}	K_{WPS}	K_{FRAC}/K_{WPS}	K_{FRAC}/K_{Ic}
Failure of cylinder (no size effect)	84 MPa.m$^{0.5}$	78 MPa.m$^{0.5}$	1.08	1.62

Table 3: Synthesis of results for WPS experiment on cracked cylinder

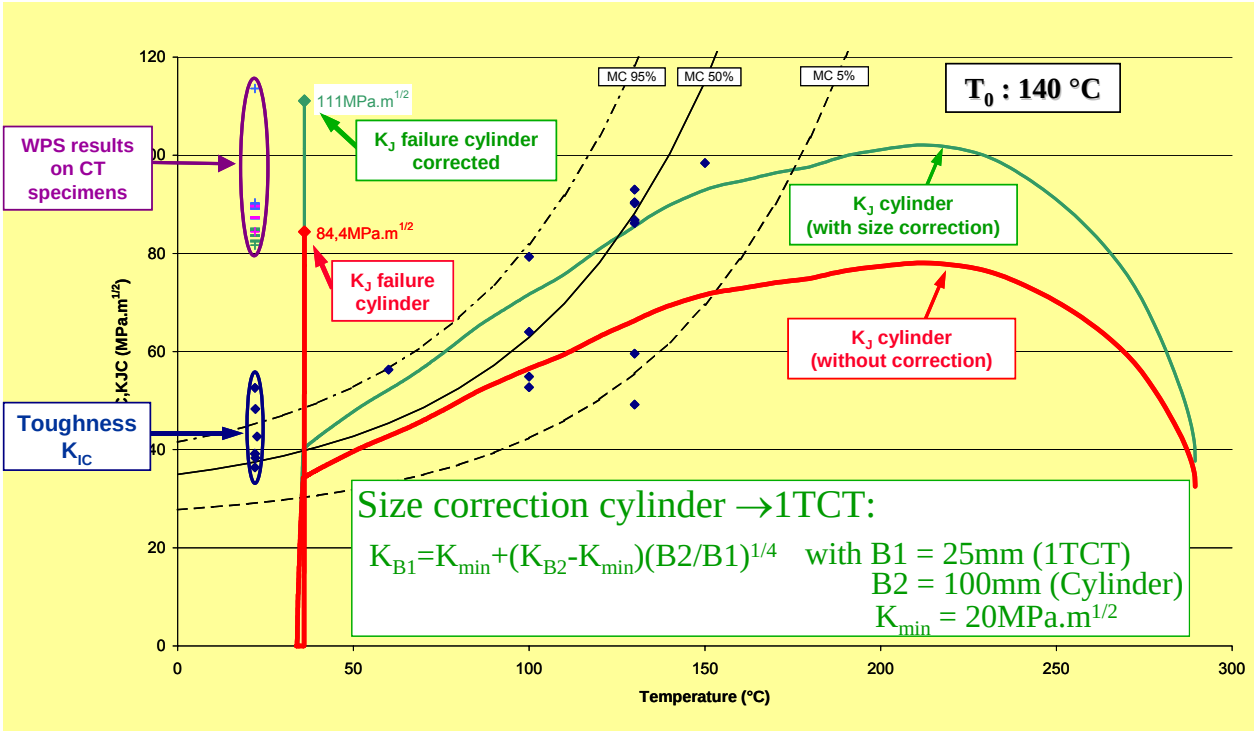

Figure 9: Synthesis of analyses for WPS experiment on cracked cylinder

The beneficial effect of warm pre-stress on material behaviour is again clearly underlined, thus confirming previous experimental results on CT specimens covering a large panel of experimental configurations (material, loading path, level of preloading …).

4.1.3 Comparison between cylinder and CT specimens (WPS3 steel)

MPA Stuttgart has also conducted additional WPS-type experiments on CT specimens on the same material WPS3 (17MoV8-4mod. steel). 1T, 2T and 4T-CT specimens have been tested, with several load paths K_J – T (LCF, LUCF, and 'Real transient') in conditions similar to the one applied on the cracked cylinder (particularly with the same level of pre-loading K_{WPS}).

Values of the SIF at fracture, K_{FRAC}, are compared to the SIF K_J of the cylinder at failure on previous figure. It appears that, in similar experimental conditions, the SIF values at final failure, K_{FRAC}, are very close between the cracked cylinder and the WPS type CT specimens.

4.2 Models to account warm pre-stress

Models to account WPS have been identified, selected and described in report [9]. This selection includes analytical or engineering models and numerical models based on refined elastic-plastic computations:

Analytical and engineering models

Chell [24][27]

Chell & Haigh [24][28]: $K_{FRAC} = K_{unload} + 0.2\ \Delta K_U + 0.87\ K_{MAT}$

Wallin [25]: $K_{FRAC} = K_{unload} + (K_{MAT} \,.\, \Delta K_U)^{0.5} + 0.15\ K_{MAT}$

where

K_{FRAC} is the predicted fracture of the specimen

K_{MAT} is the material fracture toughness at the fracture temperature

ΔK_U is the magnitude of unloading ($\Delta K_U = K_{WPS} - K_{unload}$)

Numerical models based on refined elastic-plastic computations

Generally derived from the local approach to cleavage fracture (except the energy approach), these models allow evaluating the failure probability of the specimens during the loading:

Original Beremin model [22]

$$P_f(\sigma_W) = 1 - \exp\left(-\left(\frac{\sigma_W}{\sigma_u}\right)^m\right)$$

Modified Beremin model [23]

$$P_r = 1 - e^{\left(-\int_V \left[\max_{\{u<t,\ \dot{p}(u)>0\}} \left(\frac{\sigma_I(u)}{\sigma_u(\theta(u))}\right)\right]^m \frac{dV}{V_0}\right)}$$

The key point of the model is the role of 'active plasticity' to initiate cleavage for complex loading involving unloading.

Incremental formulation of the Beremin model (proposed by IWM) [29]

$$\Delta p = \frac{\Delta \varepsilon_{pl}}{\Delta \varepsilon_{pl0}} \exp\left(-\frac{\varepsilon_{pl}}{\varepsilon_{pl0}}\right)\left(\frac{\sigma_I}{\sigma_u}\right)^m$$

The concept of 'active plasticity' is also integrated in the model.

Energy approach (G_P) [21]

$$Gp(\Delta l) = \max_{\Delta l}\left[\left(\int_{Ze}(we.dS)\right)/\Delta l\right]$$

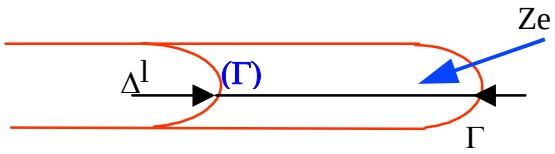

More details about the models are available in documents [9][10][14][21 to 29].

4.3 Evaluation and validation of models

WPS experiments (CT specimens, cracked cylinder) have been interpreted by partners with the panel of analyses previously mentioned. The corresponding analyses are available in report [10] (CT specimens) and [14] (cracked cylinder). Main conclusions are summarised in this section.

4.3.1 WPS experiments on CT specimens

The validation of the models is based on a comparison of the predictions given by the models with the WPS experiments results on CT specimens for LCF and LUCF loading cycles. The following figures show a synthesis of main predicted results (failure probability for numerical models, minimum and maximum predicted values for simplified approaches) compared to experimental CT experiments under monotonic loading and WPS cycles.

WPS3 material (17MoV8-4 mod. steel)

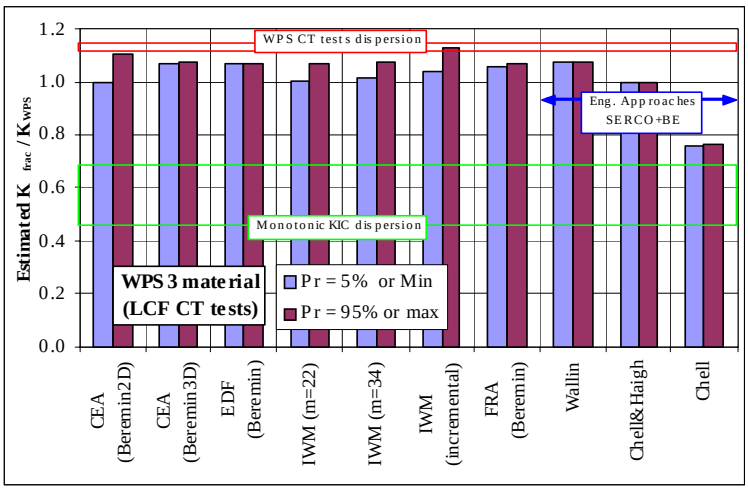

Figure 10: Synthesis of analyses on WPS3 material

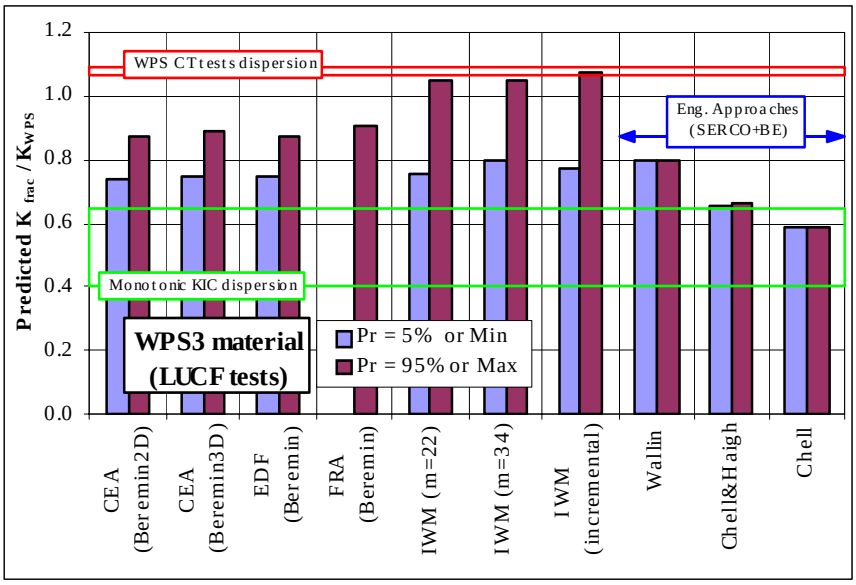

Figure 11: Synthesis of analyses on WPS3 material

18MND5 material (similar to A533 steel)

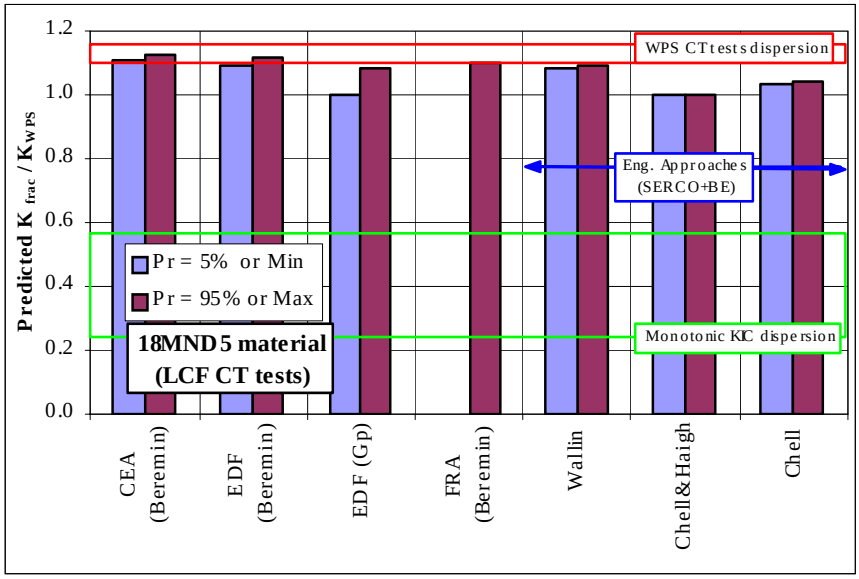

Figure 12: Synthesis of analyses on 18MND5 material

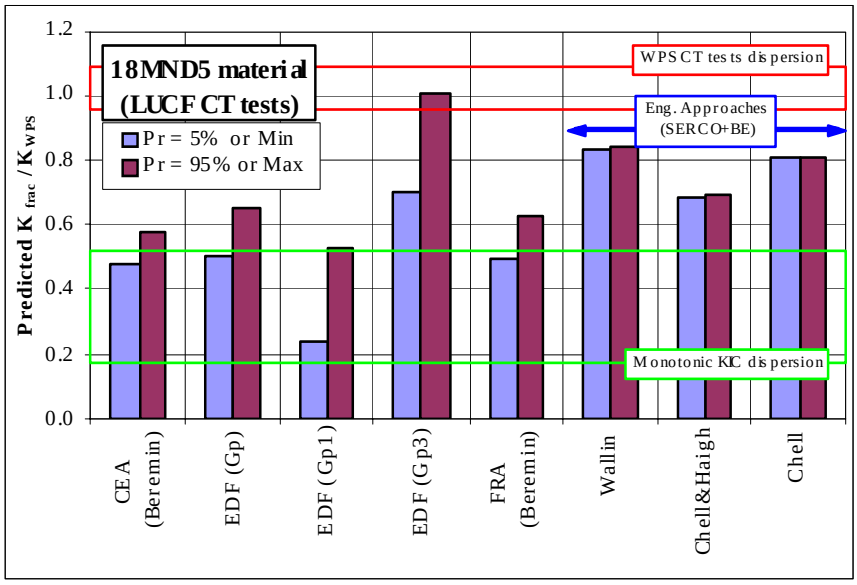

Figure 13: Synthesis of analyses on 18MND5 material

The main conclusions are summarised as follows [10]:

Engineering models

– Engineering models have the benefit of not requiring prior calibration.

– Engineering models (Chell, Chell & Haigh, Wallin) predicted the observed WPS benefit conservatively, based on the lower bound as-received fracture toughness. Based on the median as-received toughness, a few predictions exceed (by a few percent) the experimental results for LCF cycles.

– The predictions of experiments using the Wallin model are in most cases less pessimistic than those based on the Chell & Haigh model.

– The predictions of experiments using the Chell model are less pessimistic than those based on the Chell & Haigh model. However, in all cases for LUCF cycles and in nearly all cases for LCF cycles, the Chell model predicts the observed WPS benefit conservatively, based on the lower bound (5 %) master curve representation of the as-received fracture toughness. Based on the median (50 %) master curve representation, several predictions of fracture exceed, by a few percent, the corresponding values of effective fracture toughness deduced from the observation of LCF experimental results.

Numerical models based on refined elastic-plastic computations

– All partners reported comparable results for both materials in calibration of modified Beremin model (m constant, $\sigma_u(T)$).

– In all cases, application of models based on local approach to cleavage fracture predicted a beneficial effect of WPS. Agreement between analyses is excellent, in spite of the refinement of such analyses.

– In all cases, the results of LCF experiments were closely predicted.

– In all cases, the effective increase of fracture toughness shown by LUCF experiments was under predicted, mainly due to the difficulty in modelling reverse plasticity during unloading.

– Application of the Energy approach, based on the energy release rate G_P and the critical value of this parameter G_{Pc}, produced predictions of LCF and LUCF WPS experiments (on material 18MND5) comparable in accuracy with predictions deduced from the modified Beremin model.

4.3.2 WPS-type experiment on a cracked cylinder (WPS3 material)

The main results deduced from the elastic-plastic analyses are summarised on the two following figures, showing:

– a comparison between the stress-intensity factor K_J and the material fracture toughness K_{Ic} (through master curve approach with T_0: 140 °C)(without any size correction) during all the transient

– a comparison between the cylinder and WPS results obtained on CT specimens tested in similar experimental conditions

– a prediction of the experiment using the local approach to fracture (using the modified Beremin model).

These results are very satisfactory and in good agreement with the experimental observations, showing a significant increase of the component resistance regarding brittle failure (compared to the initial material fracture toughness), due to the warm pre-stress effect.

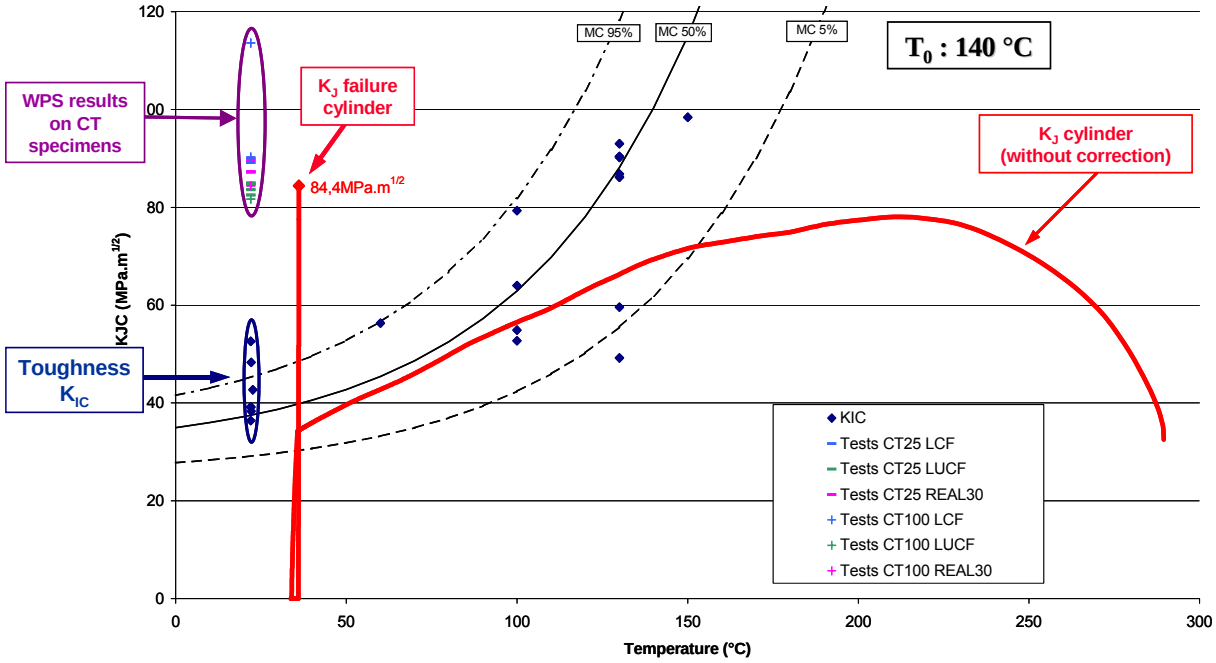

Figure 14: Synthesis of analyses on the WPS experiment on a cracked cylinder

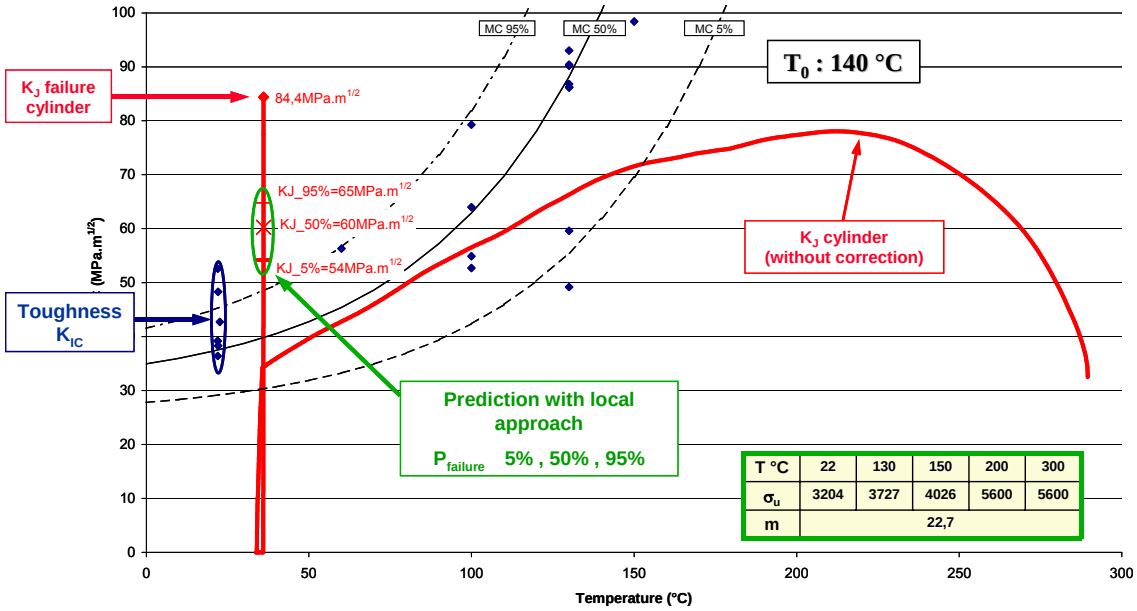

Figure 15: Synthesis of analyses on the WPS experiment on a cracked cylinder

A large panel of analyses has been used for the interpretation of the experiment, including engineering models (Chell, Haigh, Wallin), local approach to fracture (Beremin, modified Beremin, IWM incremental model) and energy approach based on G_P.

A full synthesis of analyses is available in report [14], summarised in the following figures showing:

– a comparison of the predictions from elastic-plastic analyses with the material fracture toughness (Figure 16)

– a comparison of predictions from engineering models (with several assumptions on input data) with the material fracture toughness (Figure 17)

– a comparison of all predictions to K_{Ic} material fracture toughness (Figure 18)

– a comparison of all predictions to the level of preloading K_{WPS} (Figure 19)

– a comparison of the predictions from elastic-plastic analyses with the K_{Ic} material fracture toughness.

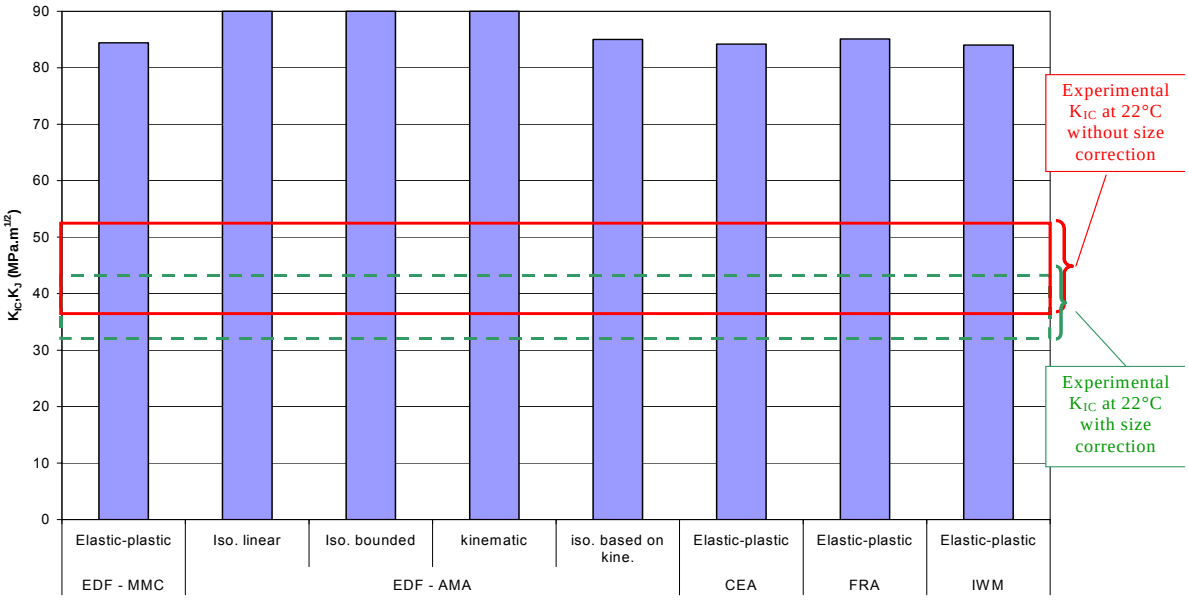

Figure 16: Comparison of elastic-plastic analyses with material fracture toughness

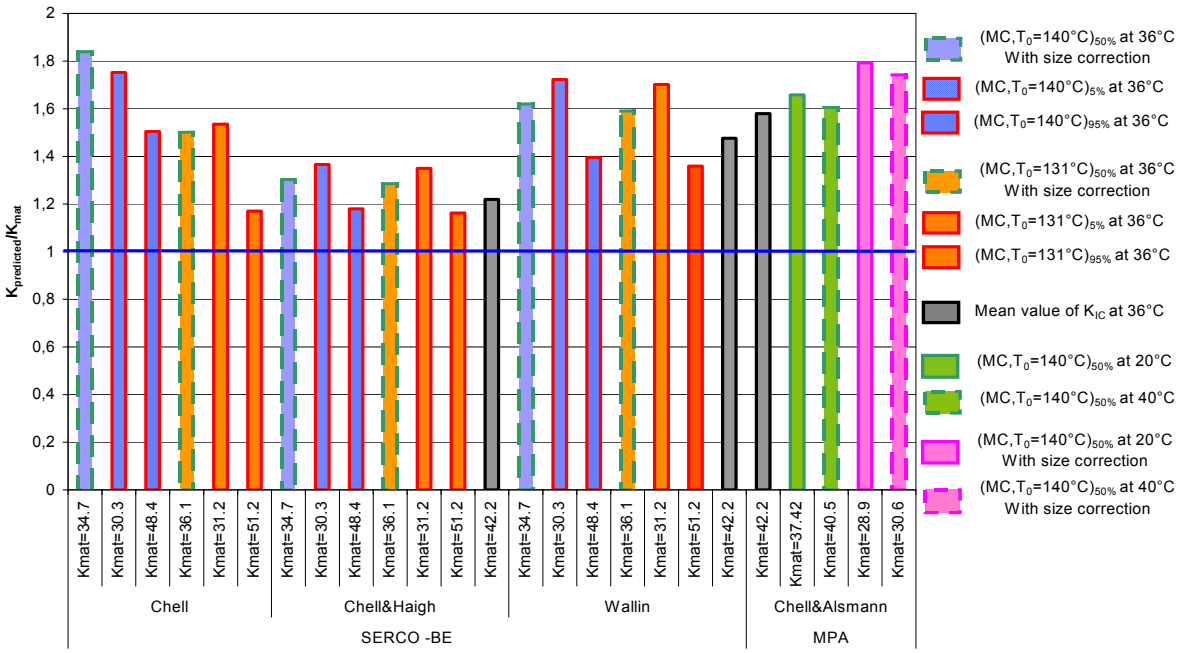

Figure 17: Comparison of engineering models with material fracture toughness

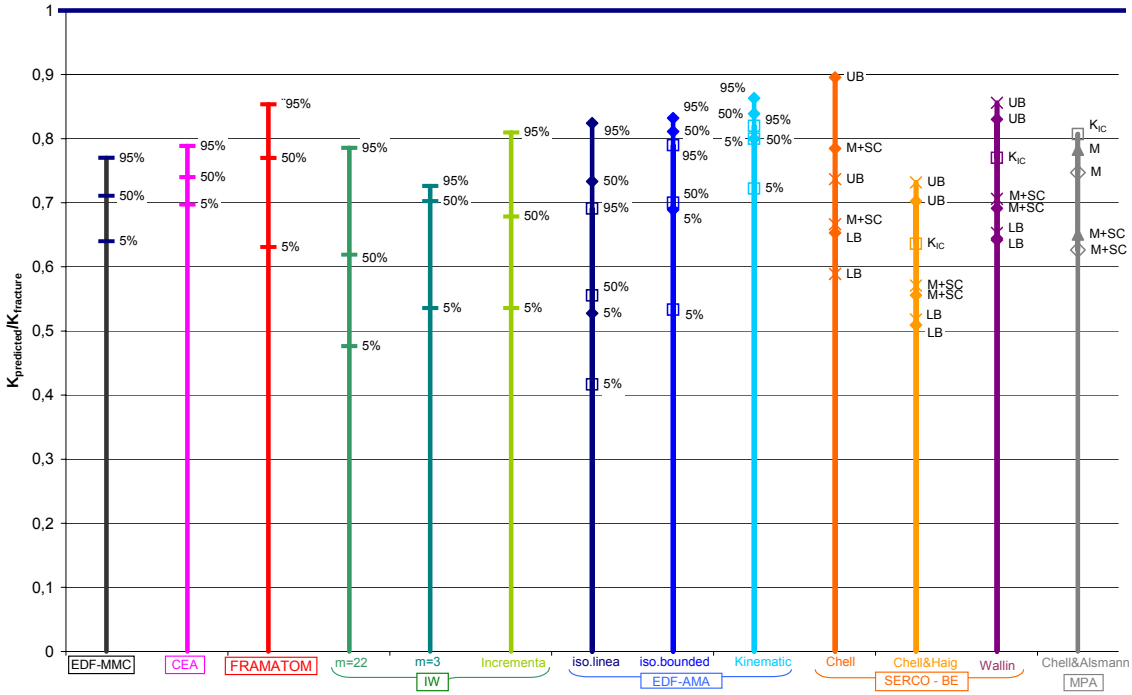

Figure 18: Comparison of all predictions to K_{Ic} material fracture toughness

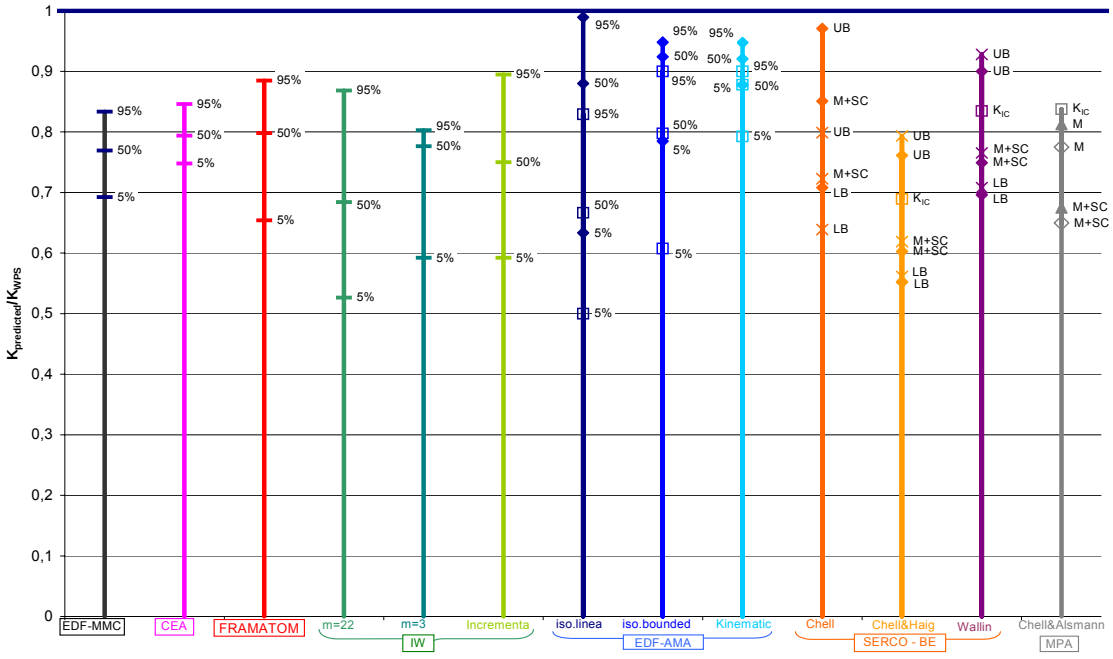

Figure 19: Comparison of all predictions to preloading K_{WPS}

The main conclusions of the analyses of the cylinder can be summarised as follows:

– All analyses, including engineering and more refined (based on elastic-plastic computations) models, are satisfactory, showing more particularly a significant increase of the resistance of the

cylinder regarding brittle failure, due to warm pre-stress effect (compared to the initial material fracture toughness).

– A good agreement between numerical finite element computations can be mentioned in the evaluation of the elastic-plastic stress-intensity factor K_J at failure.

– The capability of engineering models to demonstrate the WPS on the cylinder is also satisfactory.

– The sensitivity of engineering models to input data (mainly the material fracture toughness) is emphasised, according input data you account (lower bound, medium curve, master-curve data or effective fracture toughness at final reloading temperature).

– The agreement between the refined analyses is excellent, with very similar results (failure probability evaluation).

– The predictions of refined models based on local approach to fracture are always conservative, but this conservatism sometimes appears too high. The accuracy of such approaches could be improved.

– To conclude, all predictions are in agreement with the experimental result on the cylinder, still conservative, with a level of accuracy depending on analyses refinement and input data.

4.4 Application of models to RPV

The objective of work-package WP5 was the application of the WPS methodology – with the corresponding models – on two RPV representative cases. Two practical examples have been chosen for the demonstration, one axial surface flaw and one axial sub-surface flaw in the cylindrical part of a typical Western PWR RPV, loaded by pressure and temperature loading. All details can be found in the specifications described in report [15] (Deliverable D11). A schematic of the analysis is given in the following figure:

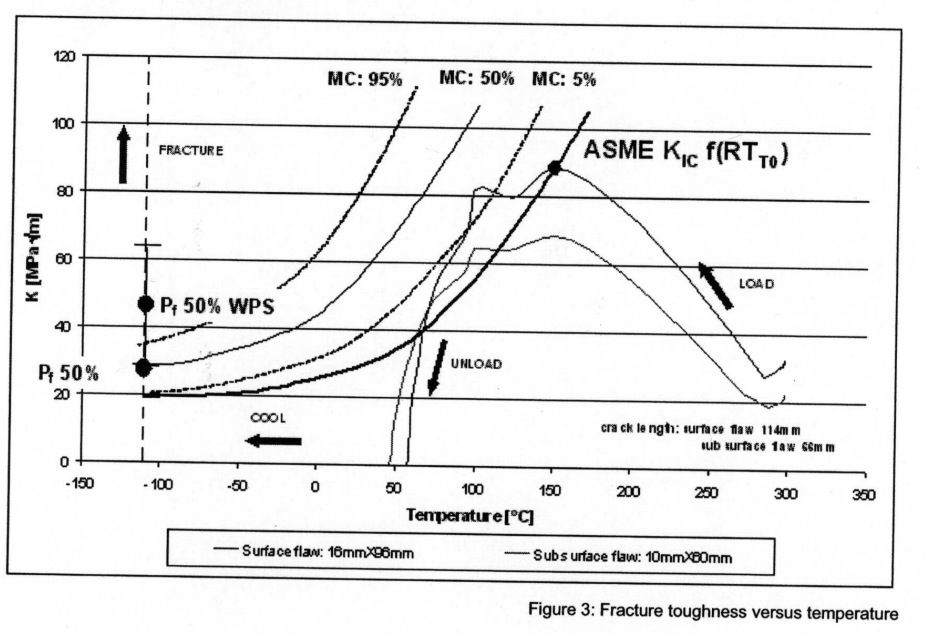

Figure 20: Schematic of the analysis

Different approaches have been applied for these applications, including analytical models (Chell, Chell & Haigh) and refined models based on local approach to fracture (IWM incremental model, modified Beremin model (Gao [30])). A synthesis of these analyses is available in document [17](Deliverables D12 & D13). The main results can be summarised as follows:

– The fracture toughness of the material after WPS is significantly increased compared to the virgin material.

– The analytical models are conservative to the results given by the local approach.

– Constraint effects of the sub-clad flaw lead to higher K_{FRAC} values compared to the surface through-clad flaw.

– WPS effect on real cases could be quantified using analytical models and local approach.

– Load calculation between the different project partners is in good agreement.

An example of application of WPS on RPV – using the local approach to fracture (Beremin model modified by Gao, [30]) – is given in the following figure:

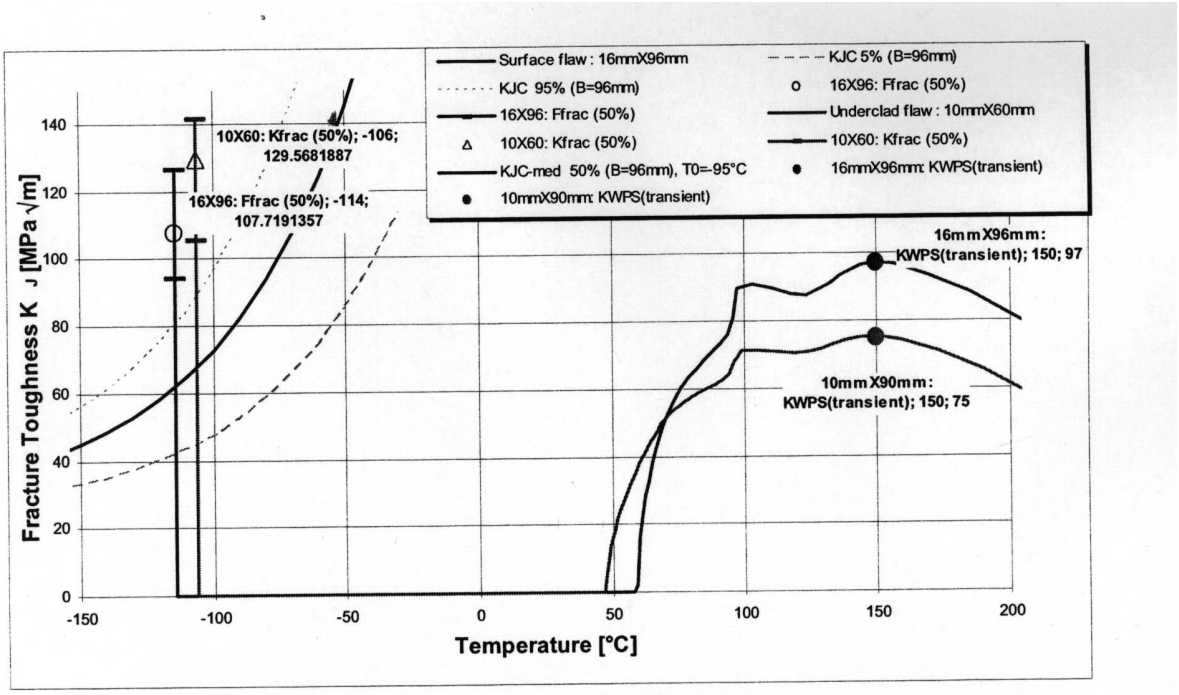

Figure 9. Results as a shift in the fracture toughness for both flaw types with transient preloading

Figure 21: Example of application of WPS on RPV

4.5 Synthesis

The experimental evidence of warm pre-stress effect on brittle failure of RPV steels has been confirmed through experiments conducted within the framework of the SMILE project:

– WPS-type experiments on classical CT specimens, with a large panel of experimental conditions

– a PTS-type transient involving WPS on a cracked cylinder, with a more complex loading.

In all cases, the results lead to the following observations:

– *No initiation occurred during unloading ($dK_J/dt < 0$), even if $K_J > K_{Ic,}$*

– *No initiation occurred during cooling under constant loading ($dK_J/dt = 0$ (e.g. LCF cycle))*

– *In case of an additional reloading at lower temperature, a significant increase of the material resistance at failure, K_{FRAC}, is obtained regarding the risk of brittle failure initiation, compared to the initial material fracture toughness K_{Ic} (in the absence of WPS), $K_{FRAC} > K_{Ic}$ or $K_{FRAC} >> K_{Ic}$ according to the loading path $K_J – T$.*

Several models are available to model and account this effect in an RPV assessment, including engineering models (Chell, Haigh, Wallin) and more refined approaches generally based on local approach to fracture.

The capability of such models to predict the main experimental results has been demonstrated, including a quantification of margins induced by the WPS effect. The corresponding predictions are still conservative, even if this conservatism sometimes seems too high.

For ‘complex loadings’ involving unloading, the role of ‘active plasticity’ to initiate brittle failure is fundamental and has been incorporated in the recent models based on local approach to cleavage fracture (modified Beremin, IWM model).

The applicability of the WPS models to real RPV assessment is also demonstrated, through two practical examples based on a typical Western PWR RPV.

5. APPLICATION OF WARM PRE-STRESS IN RPV ASSESSMENT

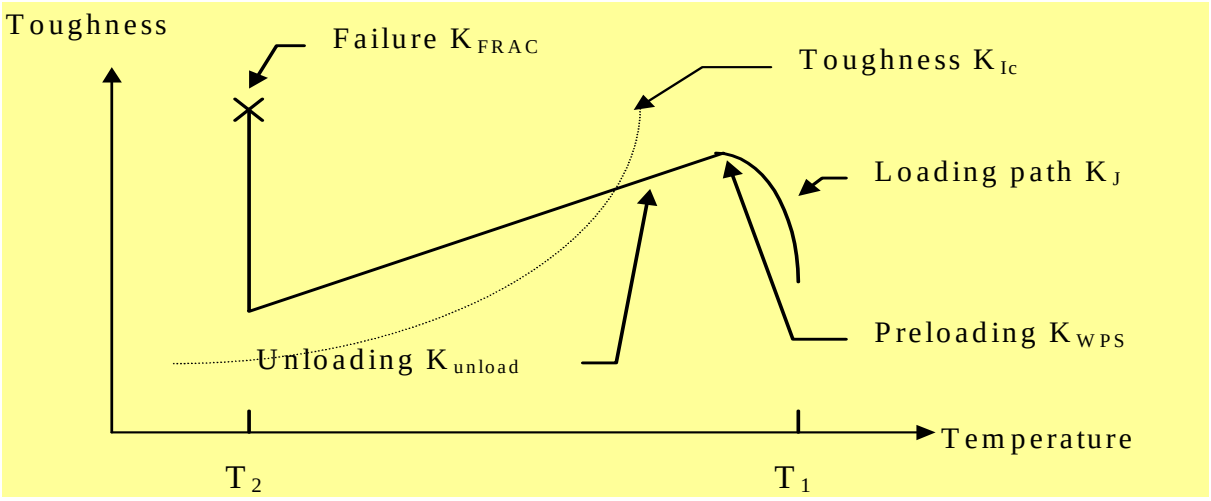

Figure 22: The WPS principle in RPV assessment

All WPS results obtained within framework of the project underline the following conclusions:

– Brittle failure initiation during a PTS event is not possible if the stress-intensity factor K_J is constant or monotonically decreasing to a value K_{unload} ($\Leftrightarrow dK_J/dt \leq 0$).

– In case of reloading at a lower temperature, T_2, additional margins occur (K_{FRAC}) regarding the risk of brittle failure initiation (due to WPS) compared to the initial material fracture toughness K_{Ic}.

– These additional margins are generally dependent on loading conditions (transient, level of preloading K_{WPS} …).

These results confirm experimental evidence of warm pre-stress effect on brittle failure of RPV ferritic steels, in full agreement with experimental results already available through the world on a large panel of experimental conditions.

5.1 Conditions for application

The following conditions, proposed in R6 – Revision 4, Section III.10.4, to apply WPS in RPV assessment [24] for a PTS-type transient are required:

– The failure mechanism at the service condition must be transgranular cleavage or intergranular brittle fracture.

– The flow properties of the material should increase between the WPS and the service failure conditions.

– There should be no significant sub-critical crack growth between the WPS and the service failure condition. The amount of any such crack growth should be much less than the extent of the residual plastic zone following unloading.

– The stress-intensity factor, K_{WPS}, due to the WPS preloading exceeds the material fracture toughness, K_{Ic}, at the reload condition.

– Small-scale yielding conditions hold, that is $(K_J/\sigma_y)^2 / 2\beta$ is much less than the size of the uncracked ligament and any relevant structural dimensions, with σ_y the yield stress at the pre-loading and $\beta = 1$ or 3 in plane stress or plane strain.

– The pre-loading and the re-loading should be in the same direction; that is, both tensile or both compressive at the crack tip. A compressive pre-loading followed by a tensile re-loading may reduce the apparent fracture toughness.

5.2 Proposal for recommendations

5.2.1 Use of WPS during unloading

If previous requested conditions are respected, WPS effect can be applied in RPV assessment during a monotonic unloading, without any additional justification:

Brittle failure initiation is not possible during a PTS event if the stress-intensity factor K_J is constant or monotonically decreasing $\Leftrightarrow$

(1) $K_J \leq K_{WPS}$ and $dK_J/dt \leq 0$

No additional condition (safety coefficient or additional margin) is required to account WPS during monotonic unloading.

5.2.2 Use of WPS during reloading

The possible application of WPS effect during an additional reloading, in a PTS type scenario, is not as comfortable as in unloading conditions, particularly to quantify margins induced by WPS. The additional margins – regarding the risk of brittle failure initiation in RPV – clearly exist as shown through available experimental, analytical, and numerical results. However, these margins can be strongly loading-dependent (loading path K_J-T, level of preloading K_{WPS} …) and the risk of brittle failure initiation is still possible with re-loading increasing. This beneficial effect cannot reasonably be included in some codes or standards, but the additional margins induced by this effect can be evaluated case by case using available corresponding models (which are fully validated).

As mentioned earlier, models to account WPS have been identified, described, evaluated, and validated [9][10][14][18][21 to 29]. They can be classified as:

– analytical or engineering models: Chell, Chell & Haigh, Wallin

– numerical models: local approach to fracture, energy approach.

Numerical models are more physically based. They have been validated within the SMILE project (both on CT and cylinder experiments). However, the application of such models is more complex (than analytical approaches) and requires more refined (elastic-plastic) computations, generally involving the identification of specific parameters (e.g. m and σ_u parameters for the Beremin model). This identification is not necessarily always easy for RPV material (e.g. irradiation effect, dependence with temperature). Nevertheless, a strong interest of such approaches is to validate analytical or engineering models. That is the case in all analyses performed in this project.

Analytical models are easier to be used to evaluate additional margins induced by WPS, even if the technical bases of such models are not so robust:

– A first model has been developed by Chell [9][14][24][27], R6 – Revision 4, Chapter III, Section III.10.

– It has been simplified in a second step by Chell and Haigh (same references) to account situations involving unloading [28]. The stress-intensity factor at failure K_{FRAC} is given in this case by the following expression (R6 – Revision 4, chapter III) (see corresponding terminology in Section 3.1):

(3) $\mathbf{K_{FRAC} = K_{unload} + 0.2\ \Delta K_U + 0.87\ K_{Ic}}$ (see corresponding terminology in Section 3.1)

– Recent developments by K. Wallin lead to the following expression of the stress-intensity factor at failure K_{FRAC} [9][10][24][25]:

(4) **If $K_{Ic} < \Delta K_u$: $K_{FRAC} = K_{unload} + (K_{Ic} \,.\, \Delta K_u)^{0.5} + 0.15\ K_{Ic}$**

(4') **If $K_{Ic} \geq \Delta K_u$, conditions are imposed in (4): $K_{unload} = K_{WPS}$ and $\Delta K_u = 0$**

If $K_{FRAC} \leq K_{Ic}$, then **no WPS effect** $\Rightarrow$ $\mathbf{K_{FRAC} = K_{Ic}}$

With $K_{FRAC} > K_I$, **WPS effect**

where $\Delta K_R = K_{FRAC} - K_{unload}$ is the additional stress-intensity factor at failure due to re-loading

The wide applicability and simplicity of the Wallin model has led to including it in the forthcoming updated version of R6 (R6 – Revision 4, Chapter III, Section III.10), replacing the expressions of Chell and Haigh and Smith and Garwood [24].

6. CONCLUSION

Started in 2002 as part of the Fifth Framework Programme of the European Atomic Energy Community (Euratom FP5), the SMILE project aimed at harmonising the different approaches to lay the basis for European Codes & Standards regarding the inclusion of warm pre-stress (WPS) in RPV assessment regarding the risk of brittle failure.

The project is achieved and all results are available on experimental, analytical, and numerical aspects. The beneficial effect of warm pre-stress on brittle failure of RPV steels has been experimentally confirmed, and the capability of some analytical, engineering, and numerical tools to predict this effect – and its consequences – has been demonstrated:

– No initiation occurred during unloading ($dK_J/dt < 0$), even if $K_J > K_{Ic}$.

– No initiation occurred during cooling under constant loading ($dK_J/dt = 0$ (e.g. LCF cycle)).

– In case of an additional reloading at lower temperature, a significant increase of material resistance at failure, K_{FRAC}, is obtained regarding the risk of brittle failure initiation compared to the initial material fracture toughness K_{Ic} (in the absence of WPS), $K_{FRAC} > K_{Ic}$ or $K_{FRAC} >> K_{Ic}$ according the loading path K_J – T.

– Validated models are available to simulate and account this effect in RPV assessment, including engineering models (Chell, Haigh, Wallin) and more refined approaches generally based on local approach to fracture.

– The applicability of such models to real Western RPV assessment has been demonstrated through two practical examples.

The role of 'active plasticity' is fundamental to account unloading during cleavage initiation process, particularly in case of complex loading involving unloading during the loading path. This effect is now included in recent refined models (modified Beremin, IWM incremental model …).

Based on these elements, some recommendations are proposed regarding application and inclusion of WPS in RPV assessment:

– In case of a PTS event on an RPV, use of WPS during a monotonic unloading can be applied without additional justification or safety margin: Brittle failure initiation is not possible during the PTS if the stress-intensity factor is monotonically decreasing or remains constant.

– WPS induces additional margins regarding brittle failure initiation (stress-intensity factor at failure K_{FRAC} > initial material fracture toughness K_{Ic}) in case of reloading at lower temperature, after previous preloading of the component. These margins are loading-dependent (loading path K_J – T, level of preloading K_{WPS} …).

– Some models, including engineering and more refined approaches, are available (with variable level of refinement and accuracy) to account WPS in RPV assessment and to quantify additional margins induced by WPS. These models are well validated on a large panel of appropriate experiments. The applicability of such models to real RPV assessment has been demonstrated.

REFERENCES

[1] SMILE project – 'Structural Margin Improvements in Age-embrittled RPVs with Load History Effects', Euratom FP5 contract FIKS-CT2001-00131

[2] SMILE mid-term report

[3] SMILE 2004 progress report

[4] SMILE D1 Deliverable: Characterisation of the material WPS3 (17 MoV 8 4 mod.)(MPA Stuttgart)

[5] SMILE D2 Deliverable: Confirmation of the WPS effect on the degraded material (17 MoV 8 4 mod.)(MPA Stuttgart)

[6] SMILE D3(a) Deliverable: Characterisation of the degraded material WPS3 and demonstration of the WPS effect (MPA Stuttgart)

[7] SMILE D3(b) Deliverable: Characterisation of the French 18MND5 RPV steel and demonstration of the WPS effect (EDF)

[8] SMILE D3(c) Deliverable: Identification of WPS calibration experiments and supporting data based on D3(a) and D3(b) (SERCO)

[9] SMILE D5 Deliverable: Selection and model description for SMILE European project (CEA)

[10] SMILE D6 Deliverable: Validation of models against existing data (SERCO & CEA)

[11] SMILE D7 Deliverable: Test specification and design of validation test (MPA Stuttgart)

[12] SMILE D8 Deliverable: Validation test (MPA Stuttgart)

[13] SMILE D9 Deliverable: Fractographic investigations of the SMILE WPS verification test (JRC-IE Petten, MPA Stuttgart & CEA)

[14] SMILE D10 Deliverable: Interpretation of validation test (EDF & MPA Stuttgart)

[15] SMILE D11 Deliverable: Definition of specifications for application cases (Framatome-ANP)

[16] SMILE D12 & D13 Deliverable: Application to a RPV subclad flaw with an actual PTS transient (Framatome-ANP)

[17] SMILE D12 & D13 Deliverable: Application to a RPV sub-clad flaw (D12) and a through clad surface flaw (D13) with an actual PTS transient (Framatome-ANP)

[18] SMILE D15 Deliverable: Conclusions and recommendations, to be published (EDF)

[19] D. Moinereau: 'WPS : Bilan des études sur le préchargement à chaud et de sa prise en compte dans l'analyse des marges des cuves REP vis-à-vis de la rupture fragile', EDF report HT-26/05/047/A

[20] D. Moinereau et al.: 'SMILE: Interpretation of WP4 PTS transient-type experiment performed on a cracked cylinder involving warm pre-stress', SMIRT 18 conference, Beijing, 7-12 August 2005

[21] Y. Wadier: 'The energy approach of elastic-plastic fracture mechanics applied to the analysis of a WPS experiment on a cracked cylinder', ASME Pressure Vessels and Piping Conference, Denver, USA, 17-21 July 2005

[22] F. Mudry: 'A local approach to cleavage fracture', International Seminar on Local Approach to Fracture, Moret-sur-Loing, France, 3-5 June 1986

[23] R. Masson et al.: 'A modified Beremin model to simulate the warm pre-stress effect', *Journal of Nuclear Engineering and Design*, 216, pp. 27-42, 2002

[24] P. J. Budden: ‘Validation of the warm pre-stress effect using SMILE data’, SMILE deliverable, November 2004

[25] K. Wallin: ‘Master curve implementation of the warm pre-stress effect’, *Engineering Fracture Mechanics* 70, 2003

[26] D. Moinereau et al.: ‘SMILE project. The effect of warm pre-stress in RPV assessment : synthesis of experimental results and analyses, ASME Pressure Vessels and Piping Conference, Vancouver, Canada, 23-27 July 2006

[27] G. G. Chell: ‘Some fracture mechanics applications of warm pre-stressing to pressure vessels’, 4th International Conference on Pressure Vessel Technology, Vol. 1, 117-124, 1980

[28] G. G. Chell, J.R. Haigh: ‘The effect of warm pre-stressing on proof tested pressure vessels’, *International Journal of Pressure Vessel and Piping*, 23, 121-132, 1986

[29] H. Stockl, R. Boschen, W. Schmitt, I. Varfolomeyev, J.H. Chen: ‘Quantification of the warm prestressing effect in a shape welded 10MnMoNi5-5 material’, *Engineering Fracture Mechanics* 67, 119-137, 2000

[30] X. Gao, C. Ruggieri, R.H. Dodds: ‘Calibration of Weibull stress parameters using fracture toughness data’, *International Journal of Fracture*, 92, 175-200

[31] E. Keim, H. Schnabel, R. Langer, R. Bartsch: ‘Warm pre-stress effect measured at irradiated RPV weld material’, 2005 ASME PVP Conference, 17-21 July 2005, Denver, USA

[32] D. Moinereau, A. Dahl, G. Chas, N. Rupa, J. Bourgoin, H. Churier-Bossennec: ‘Application of warm pre-stress to RPV assessment’, Fontevraud 6, 18-22 September 2006, Fontevraud, France